Enhanced Kondo Effect via Tuned Orbital Degeneracy in a Spin 1/2 Artificial Atom

S. Sasaki,[1,*] S. Amaha,[2] N. Asakawa,[2] M. Eto,[3] and S. Tarucha[1,2,4]

[1]*NTT Basic Research Laboratories, NTT Corporation, Atsugi-shi, Kanagawa 243-0198, Japan*
[2]*Department of Physics, University of Tokyo, Bunkyo-ku, Tokyo 113-0033, Japan*
[3]*Faculty of Science and Technology, Keio University, Kohoku-ku, Yokohama 223-8522, Japan*
[4]*Mesoscopic Correlation Project, ERATO, JST, Atsugi-shi, Kanagawa 243-0198, Japan*

(Received 12 November 2003; published 2 July 2004)

A strong Kondo effect is observed for a vertical quantum dot holding an odd number of electrons and spin 1/2 when an orbital degeneracy is induced by magnetic field. The estimated Kondo temperature for this "doublet-doublet" degeneracy is similar to that for the singlet-triplet degeneracy with an even electron number, indicating that a total of fourfold spin and orbital degeneracy accounts for the enhancement of the Kondo temperature. The experimental observation is qualitatively reproduced by scaling calculations using an SU(4) model at the orbital degeneracy.

DOI: 10.1103/PhysRevLett.93.017205 PACS numbers: 75.20.Hr, 73.23.Hk, 73.63.Kv

A quantum dot offers unprecedented opportunities of realizing and manipulating a single magnetic impurity interacting with a Fermi sea of conduction electrons. Rich aspects of the Kondo physics [1] have been explored owing to the tunability of relevant parameters in quantum dots. Pioneering works on the Kondo effect in quantum dots [2–6] proceed within the framework of the conventional spin 1/2 Anderson impurity model for a spin-degenerate single level. The Kondo effect is observed only when the number of electrons, N, is odd with a spin $S = 1/2$. However, exceptions to this odd-even parity behavior have been noted in a lateral quantum dot [7] where the Kondo effect is observed for both odd and even N. This has been followed by a more detailed report of the Kondo effect for even N in a "vertical" quantum dot having well-defined N and S [8]. This novel Kondo effect occurs when a magnetic field induces a spin singlet ($S = 0$)-triplet ($S = 1$) degeneracy in the multi-orbital ground state [9–15].

In this Letter, we present a new multilevel mechanism which enhances the Kondo temperature, T_K, using a vertical quantum dot. We observe a strong Kondo effect when a magnetic field induces an orbital degeneracy for odd N and $S = 1/2$. The estimated T_K is similar to that for the singlet-triplet (S-T) Kondo effect for even N, indicating that a total of fourfold spin and orbital degeneracy for both cases contributes to enhance T_K.

It is known that the orbital degeneracy plays an important role in the Kondo effect of magnetic impurities with f electrons. When the total degeneracy factor is N_d for spin and orbital degrees of freedom, the Kondo effect is described by the Coqblin-Schrieffer model of SU(N_d) symmetry [16]. The factor N_d increases T_K as $\sim D_0 e^{-1/N_d \nu J}$ with exchange coupling J, where D_0 and ν are the bandwidth and density of states of conduction electrons. We examine a model which has the SU(4) symmetry at the orbital degeneracy, yielding a larger T_K than in a single-orbital case of SU(2) symmetry, explaining the experimental results [17].

The inset of Fig. 1 schematically shows the vertical quantum dot structure used in the present study. It is in the form of a submicron-sized circular mesa fabricated from an AlGaAs/InGaAs/AlGaAs double barrier structure. Current flows vertically through the mesa, and N is changed with a gate electrode wrapped around the mesa. S and N can be unambiguously determined in this type of vertical quantum dots owing to the highly symmetric lateral confinement potential and a built-in dot-lead coupling Γ via AlGaAs barriers [18]. Γ for the present dot device is 400 μeV for the first electron entering the dot and gradually increases as N increases. All the transport measurements have been performed in a dilution

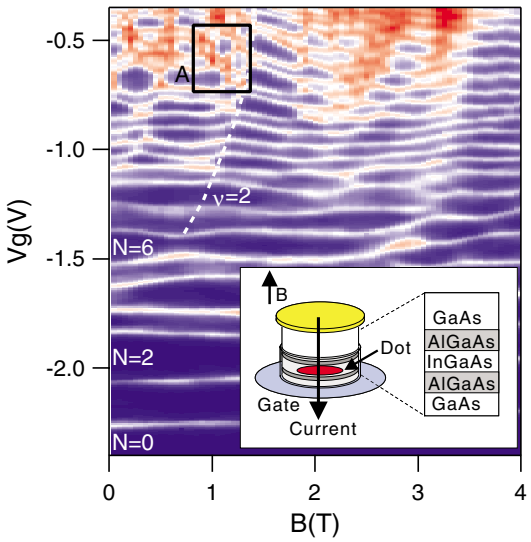

FIG. 1 (color). Color-scale plot of the linear conductance as a function of the gate voltage and magnetic field. Blue corresponds to zero conductance, white to $G = 25$ μS, and red to $G = 50$ μS. All the electrons occupy the first Landau level on the right-hand side of the dashed line (filling factor $\nu = 2$). The inset shows a schematic diagram of the dot structure made from AlGaAs/InGaAs/AlGaAs double barrier tunnel diode.

refrigerator with a base temperature of $\simeq 60$ mK, using a standard lock-in technique with an ac excitation voltage between the source and drain of 3 μV. We apply a magnetic field parallel to the current.

Figure 1 shows a color-scale plot of the linear conductance, G, as a function of gate voltage, V_g, and magnetic field, B, at base temperature $\simeq 60$ mK. Conductance shows maxima at specific V_g where N is allowed to change by one for a fixed B (Coulomb oscillation peaks). Therefore, each stripe in Fig. 1 represents a B dependence of the N-electron ground state. Large Coulomb blockade gaps at $N = 2$ and 6 at $B = 0$ reflect the shell filling of $1s$ and $2p$ orbital states, respectively, formed in a disk-shaped circular artificial atom [18]. Overall evolution of stripes with B agrees with successive filling of the single particle levels, or Fock-Darwin states [19] $E_{n,l}$, by spin-up and spin-down electrons. $E_{n,l}$ is shown in Fig. 2(a);

$$E_{n,l} = -\frac{l}{2}\hbar\omega_c + \left(n + \frac{1}{2} + \frac{1}{2}|l|\right)\hbar\sqrt{4\omega_0^2 + \omega_c^2}, \quad (1)$$

where $n = 0, 1, 2, \ldots$ is the radial quantum number and $l = 0, \pm 1, \pm 2, \ldots$ is the angular quantum number. $\hbar\omega_0$ is the lateral confinement energy and $\hbar\omega_c = eB/m^*$. The pairwise motion of the stripes in Fig. 1 is due to the spin degeneracy of each $E_{n,l}$ state.

When the Kondo effect occurs at $T \leq T_K$, the conductance in the Coulomb blockade gap increases. In our quantum dot device, Γ gradually increases with increasing V_g. Therefore, T_K generally increases as V_g increases, and the enhancement of the conductance due to the Kondo effect is noticeable in the Coulomb blockade gaps for $V_g > -1.0$ V.

The solid lines in Fig. 2(b) schematically show a magnetic field dependence of the electrochemical potential for electron numbers from $N + 1$ (odd) to $N + 4$ (even) when electrons are added to the two crossing orbitals. Coulomb interaction favors a spin triplet state ($S = 1$) for $N + 2$ in the vicinity of the magnetic field where a single particle level crossing occurs, and the ground state shows a downward cusp [20]. The S-T Kondo effect is expected on the dotted lines with a considerably higher Kondo temperature, $T_K^{\text{S-T}}$, than the conventional $S = 1/2$ Kondo temperature, T_K^D, because of the larger degeneracy [8].

Figure 2(c) shows detailed measurement conducted in region A marked in Fig. 1. The last orbital crossings occur between $E_{n,l}$ states with $(n, l) = (0, -1)$ and $(0, l)$ $(l > 1)$ on the dotted line, and all the electrons occupy the ground Landau level at higher B ($\nu = 2$). A spin triplet state is observed at $N = 16$ and $B \simeq 1.2$ T, where states $(n, l) = (0, -1)$ and $(0, 7)$ are occupied by electrons having parallel spins [see circle in Fig. 2(a)]. In the $N = 16$ Coulomb blockade gap, the conductance is enhanced by the S-T Kondo effect at $B \simeq 1.1$ and $B \simeq 1.3$ T, corresponding to the dotted lines in Fig. 2(b). As for $N = 15$ and 17, the conventional $S = 1/2$ Kondo effect is expected. However,

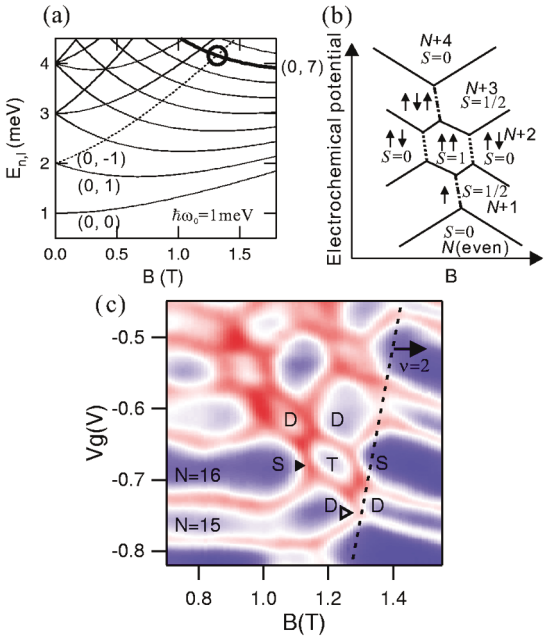

FIG. 2 (color). (a) Fock-Darwin states calculated with $\hbar\omega_0 = 1$ meV. The circle denotes crossing between orbital state $(n, l) = (0, -1)$ (dotted line) and (0, 7) (thick solid line) where the Kondo effect for $N = 15$ and 16 is studied in detail. (b) Schematic magnetic field dependence of the electrochemical potential for electron numbers from $N + 1$ (odd) to $N + 4$ (even) occupying two crossing orbitals. A skew toward the upper-left direction takes into account the effect of decreasing $\hbar\omega_0$ with increasing N. (c) Detailed measurement conducted in region A in Fig. 1. The color scale is same as in Fig. 1. S, T, and D denote states with $S = 0$ (singlet), $S = 1$ (triplet), and $S = 1/2$ (doublet).

the conductance enhancement in the Coulomb blockade gaps is not clearly observed except in the regions corresponding to the dash-dotted lines in Fig. 2(b), where two $S = 1/2$ states with different total angular momentum, M, are degenerate. When such an orbital degeneracy is present for odd N, a total of four states, i.e., $M = M_1, M_2$ $(M_1 \neq M_2)$, $S_Z = \pm 1/2$, are involved in forming the Kondo singlet state (if one can neglect the Zeeman splitting), and enhancement of T_K similar to the S-T Kondo effect is expected. We define this new multilevel mechanism for odd N as "doublet-doublet" (D-D) Kondo effect. Because T_K^{D} is much lower than the D-D Kondo temperature, $T_K^{\text{D-D}}$, only a slight conductance enhancement is observed in the odd N Coulomb blockade regions when there is no orbital degeneracy. Then, a honeycomb pattern is formed in a B-N diagram, as is clearly captured in Fig. 2(c), due to the S-T and D-D Kondo effects that occur consecutively for different orbital crossings, provided $T_K^{\text{D}} < T < T_K^{\text{S-T}}$, $T_K^{\text{D-D}}$. Our honeycomb pattern is different from the "chessboard pattern" discussed in a lateral quantum dot [21]. In a vertical quantum dot, one can assume that the orbital quantum numbers are conserved in tunnel processes between the dot and leads due to their same rotational symmetry. Hence we expect "two

channels'' of conduction electrons in the leads when two orbitals are relevant in the quantum dot; each channel couples to only one of the two orbitals. In a lateral quantum dot, on the other hand, a ''single channel'' in the leads preferentially couples to the outer orbital in the dot.

Figure 3(a) shows temperature dependence of the differential conductance dI/dV_{sd} versus V_{sd} for the S-T ($N = 16$) and D-D ($N = 15$) Kondo effect [solid and open triangle in Fig. 2(c), respectively] with the gate voltage fixed in the center of the respective Coulomb blockade gap. A clear Kondo peak at $V_{sd} = 0$ is observed at low temperatures, whose height decreases with increasing temperature as expected for the Kondo effect. Temperature dependence of the Kondo peak height normalized by the low temperature limit value, G_0, is shown in Fig. 3(b). A background from non-Kondo cotunneling is subtracted from each trace in Fig. 3(a) [22]. The Kondo peak conductance shows almost linear log$T$ dependence around $\simeq$400 mK and saturates at lower a temperature. The unitary limit conductance of $2e^2/h$ [23] is not reached in our device probably because of the asymmetry in the two tunnel barriers. Dotted lines in Fig. 3(b) are the theoretical curves

$$G/G_0 = \{T_K'^2/(T^2 + T_K'^2)\}^s, \qquad (2)$$

fitted to the data, where $T_K' = T_K/\sqrt{2^{1/s} - 1}$ [4,24]. The T_K for the S-T and D-D Kondo effect estimated from the curve fitting are 700 mK and 490 mK, respectively. The higher T_K for the S-T Kondo effect may be due to the larger Γ, and it is difficult to experimentally determine which is larger, $T_K^{\text{S-T}}$ or $T_K^{\text{D-D}}$, for the same Γ. The fitted values of the parameter s are larger than $s \simeq 0.2$ for a conventional spin 1/2 system. However, the estimation of s is less reliable because it changes substantially with the chosen fitting range. The expected Zeeman splitting of $\simeq 30\ \mu$eV at $B \simeq 1.2$ T is smaller than T_K estimated above. Therefore, no Zeeman splitting of the dI/dV_{sd} Kondo peak is observed, and we treat all four S-T and D-D states as quasidegenerate.

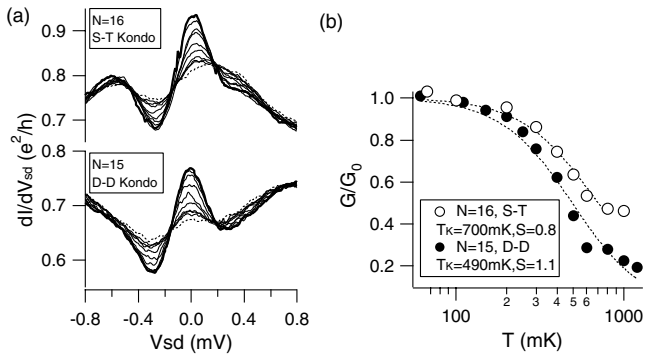

FIG. 3. (a) Temperature dependence of the differential conductance dI/dV_{sd} versus V_{sd} for the S-T and D-D Kondo effect from $T = 60$ mK (thick solid line) to 1.5 K (dashed line). (b) Temperature dependence of the Kondo peak height normalized by the low temperature limit value. Dashed lines are the theoretical curves fitted to the data.

Next, let us investigate the effect of lifting the S-T and D-D degeneracy by changing B. Figures 4(a) and 4(b) show a color-scale plot of dI/dV_{sd} in B-V_{sd} plane for the D-D Kondo effect ($N = 15$) and for the S-T Kondo effect ($N = 16$), respectively, with V_g fixed in the center of the respective Coulomb blockade gap. Conductance peaks at $V_{sd} = 0$ are observed near the degeneracy field, B_0. Because the S-T or D-D degeneracy is lifted as $|\Delta B| = |B - B_0|$ increases, the Kondo effect is broken and the zero-bias peak is suppressed. At large $|\Delta B|$, a peak or step is observed at $eV_{sd} = \pm\Delta$, where the color suddenly changes. Here, Δ is the B-dependent energy difference between the singlet and triplet states, or between the two doublet states. This peak/step is due to cotunneling associated with the two states separated by Δ [8], and therefore observed within the Coulomb blockade gap ($\simeq$0.6 meV).

Figure 4(c) shows V_{sd} values of the conductance peak/step as a function of ΔB. Peak/step positions for the S-T ($B_0 = 1.12$ T) and the D-D ($B_0 = 1.25$ T) Kondo effect

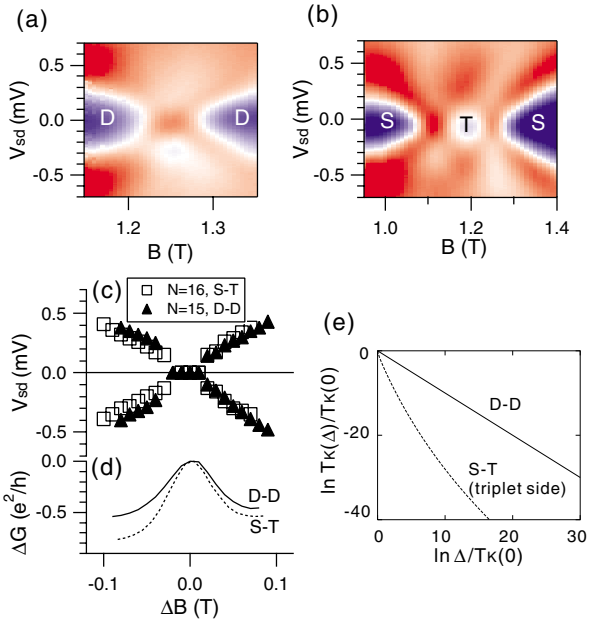

FIG. 4 (color). Color-scale plot of dI/dV_{sd} in B-V_{sd} plane for (a) the $N = 15$ D-D Kondo effect and (b) the $N = 16$ S-T Kondo effect with V_g fixed in the center of the respective Coulomb blockade gap. Blue corresponds to $G = 10\ \mu$S and red to $G = 35\ \mu$S. (c) V_{sd} values of the conductance peak or step obtained from (a) and (b) as a function of the magnetic field difference $\Delta B = B - B_0$, where B_0 is the degeneracy magnetic field. (d) Relative conductance measured from the degeneracy ($\Delta B = 0$) at $V_{sd} = 0$, for the D-D (solid line) and the S-T (dotted line) Kondo effect. (e) Calculated results of $T_K/T_K(0)$ as a function of $\Delta/T_K(0)$, on a log-log scale. $T_K(0)$ is the Kondo temperature at $\Delta = 0$. For the S-T Kondo effect (triplet side), $T_K(\Delta)$ deviates from a power law for large Δ (see Ref. [10]; we choose $J_1 = J_2$ and $C_2 = 0$).

almost coincide, indicating that they involve the same orbital states, namely, $(n, l) = (0, -1)$ and $(0, 7)$.

For the D-D Kondo effect, we examine an SU(4) model. The dot state is characterized by spin $S_z = \pm 1/2$ and pseudospin $T_z = \pm 1/2$ corresponding to two orbitals, $\mu = (S_z, T_z)$. Considering the second-order tunneling processes to the leads with two channels [25], we obtain

$$H = \sum_{k,\mu} \varepsilon_k c^\dagger_{k,\mu} c_{k,\mu} + J\mathbf{S}\cdot\mathbf{s} + \tilde{\mathbf{B}}\cdot\mathbf{S}, \tag{3}$$

with $\mathbf{S} = \frac{1}{2}\sum_{\mu\nu} d^\dagger_\mu \hat{\mathbf{\Sigma}}_{\mu\nu} d_\nu$, $\mathbf{s} = \frac{1}{2}\sum_{kk'}\sum_{\mu\nu} c^\dagger_{k',\mu} \hat{\mathbf{\Sigma}}_{\mu\nu} c_{k,\nu}$, where $d^\dagger_\mu$ and d_μ ($c^\dagger_{k,\mu}$ and $c_{k,\mu}$) are the creation and annihilation operators of dot state μ (conduction electron k, μ). Fifteen components of $\hat{\mathbf{\Sigma}}$ are generators of the Lie algebra Su(4), $\{(\sigma_x, \sigma_y, \sigma_z, I) \otimes (\rho_x, \rho_y, \rho_z, I)\} - \{I \otimes I\}$, where σ_i (ρ_i) are the Pauli matrices in the spin (pseudospin) space and I is the unit matrix. The energy difference Δ is expressed by the fictitious magnetic field $\tilde{\mathbf{B}}$, the $I \otimes \rho_z$ component of which is Δ and the other components are 0 [$\tilde{\mathbf{B}}\cdot\mathbf{S} = (\Delta/2)\sum_{S_z}(d^\dagger_{S_z,1/2} d_{S_z,1/2} - d^\dagger_{S_z,-1/2} d_{S_z,-1/2})$].

We evaluate T_K as a function of Δ using the "poor man's" scaling method [26]. We find that (i) $T_K(\Delta)$ is maximal around $\Delta = 0$, and (ii) $T_K(\Delta)$ decreases with increasing Δ by a power law, $T_K(\Delta) = T_K(0) \times [T_K(0)/\Delta]^\gamma$ with $\gamma = 1$ [27]. In the S-T Kondo effect, $T_K(\Delta)$ obeys a power law with $\gamma = 2 + \sqrt{5}$ on the triplet side, whereas $T_K(\Delta)$ drops to zero suddenly on the singlet side [10,12]. Figure 4(d) shows the experimentally observed relative conductance, ΔG, measured from the degeneracy ($\Delta B = 0$) at $V_{\rm sd} = 0$, as a function of ΔB. The conductance drops abruptly on the singlet side ($\Delta B < 0$) in the S-T Kondo effect, whereas it drops more slowly and symmetrically in the D-D Kondo effect, in qualitative agreement with the theory [Fig. 4(e)]. These behaviors are also present for other D-D and S-T Kondo effects at different N, shown in Fig. 2(c).

In summary, we have presented a new multilevel mechanism for the Kondo effect in an artificial atom. We have shown that an orbital degeneracy for odd N and $S = 1/2$ dramatically enhances the Kondo effect as in the S-T Kondo effect reported before.

The authors acknowledge valuable discussions with T. Sato, W. Izumida, L. I. Glazman, H. Hyuga, M. Stopa, and J. Kondo. The work is supported by the financial support from the Grant-in-Aid for Scientific Research A (Grant No. 40302799), the Nano-Photonic and Electron Devices Technology Project, the Focused Research and Development Project for the Realization of the World's Most Advanced IT Nation, and SORST-JST.

The power law of $T_K(\Delta)$ in D-D Kondo effect was originally derived by K. Yamada *et al.* [28].

*Electronic address: satoshi@nttbrl.jp

[1] J. Kondo, Prog. Theor. Phys. **32**, 37 (1964).
[2] D. Goldhaber-Gordon *et al.*, Nature (London) **391**, 156 (1998).
[3] S. M. Cronenwett *et al.*, Science **281**, 540 (1998).
[4] D. Goldhaber-Gordon *et al.*, Phys. Rev. Lett. **81**, 5225 (1998).
[5] J. Schmid *et al.*, Physica (Amsterdam) **256B-258B**, 182 (1998).
[6] F. Simmel *et al.*, Phys. Rev. Lett. **83**, 804 (1999).
[7] J. Schmid *et al.*, Phys. Rev. Lett. **84**, 5824 (2000).
[8] S. Sasaki *et al.*, Nature (London) **405**, 764 (2000).
[9] M. Eto and Yu. V. Nazarov, Phys. Rev. Lett. **85**, 1306 (2000); M. Eto and Yu. V. Nazarov, Phys. Rev. B **64**, 85 322 (2001).
[10] M. Eto and Yu. V. Nazarov, Phys. Rev. B **66**, 153319 (2002).
[11] M. Pustilnik, Y. Avishai, and K. Kikoin, Phys. Rev. Lett. **84**, 1756 (2000).
[12] M. Pustilnik and L. I. Glazman, Phys. Rev. Lett. **85**, 2993 (2000); M. Pustilnik and L. I. Glazman, Phys. Rev. B **64**, 045328 (2001).
[13] D. Giuliano and A. Tagliacozzo, Phys. Rev. Lett. **84**, 4677 (2000).
[14] D. Giuliano *et al.*, Phys. Rev. B **63**, 125318 (2001).
[15] W. Izumida *et al.*, Phys. Rev. Lett. **87**, 216803 (2001).
[16] A. C. Hewson, *The Kondo Problem to Heavy Fermions* (Cambridge University Press, Cambridge, England, 1993).
[17] For previous work of the multi-orbital Kondo effect in quantum dots, see T. Inoshita *et al.*, Phys. Rev. B **48**, 14 725 (1993); T. Pohjola *et al.*, Europhys. Lett. **40**, 189 (1997); W. Izumida *et al.*, J. Phys. Soc. Jpn. **67**, 2444 (1998); A. Levy Yeyati *et al.*, Phys. Rev. Lett. **83**, 600 (1999).
[18] S. Tarucha *et al.*, Phys. Rev. Lett. **77**, 3613 (1996).
[19] V. Fock, Z. Phys. **47**, 446 (1928); C. G. Darwin, Proc. Cambridge Philos. Soc. **27**, 86 (1930).
[20] S. Tarucha *et al.*, Phys. Rev. Lett. **84**, 2485 (2000).
[21] M. Stopa *et al.*, Phys. Rev. Lett. **91**, 046601 (2003), and references therein.
[22] L. I. Glazman and M. Pustilnik, in *New Directions in Mesoscopic Physics*, NATO ASI (Kluwer, Erice, 2002).
[23] W. G. van der Wiel *et al.*, Science **289**, 2105 (2000).
[24] T. A. Costi and A. C. Hewson, Philos. Mag. B **65**, 1165 (1992).
[25] We assume that the strength of the tunnel coupling V is equivalent for two orbitals, which seems to be the experimental situation. The exchange coupling J in Eq. (3) is given by $J = V^2/E_c$, where $1/E_c = 1/E^+ + 1/E^-$ with $E^\pm$ being addition and extraction energies.
[26] We obtain scaling equations (i) $dJ/d\ln D = -4\nu J^2$ for the energy scale $D \gg \Delta$ [SU(4) Kondo effect], and (ii) $dJ/d\ln D = -2\nu J^2$ for $D \ll \Delta$ [conventional SU(2) Kondo effect]. ν is the density of states in the leads. When $\Delta \gg T_K(0)$, we match the solutions of (i) and (ii) at $D \approx \Delta$ [9,10] and obtain a power law of $T_K(\Delta)$.
[27] An equivalent situation to our SU(4) model has been examined for a double quantum dot system without interdot tunnel coupling; L. Borda *et al.*, Phys. Rev. Lett. **90**, 026602 (2003).
[28] K. Yamada *et al.*, Prog. Theor. Phys. **71**, 450 (1984).